Low-cost, thin-film, mass-manufacturable carbon electrodes for detection of t neurotransmitter dopamine

Stuart Hannah [a], Maha Al-Hatmi [a], Louise Gray [b 1] and Damion K. Corrigan [a]*

[a] Department of Biomedical Engineering, University of Strathclyde, 40 George Street G1 1QE, United Kingdom. [b] FlexMedical Solutions, Eliburn Industrial Park, Livingston, EH54 6GQ, United [1] Present address : Department of Biomedical Engineering, University of Strathclyde, 40 George Street, Glasgow, G1 1QE, United Kingdom.

- Corresponding Author : damion.corrigan@strath.ac.uk (Damion Corrigan)

KEYWORDS: Biosensors; Electrochemistry; Dopamine; Carbon; Electrodes

ABSTRACT

A flexible, thin-film carbon electrode is reported for detection of the key neurotransmitt dopamine using standard electroanalytical techniques of cyclic voltammetry, differenti voltammetry and square wave voltammetry. The thin-film electrode has been expl possible low-cost solution to detect low concentrations of dopamine and its performance ha been compared with a commercially available screen printed carbon electrode. It was found the thin-film electrode is more sensitive than the screen printed electrode, and can faithfull detect dopamine between 50 pM and 1 mM concentrations. The electrode provides a l detection of ~ 50 pM, displays good selectivity between dopamine and ascorbic acid, and

to show a level of differentiation between the two compounds in terms of peak currents as well as oxidative potentials at physiologically relevant concentrations. This is in contrast to the screen printed electrode which is unable to discriminate between dopamine and ascorbic acid at the same concentrations. The key advantages of the presented electrode system are its low-cost, flexible substrate, and the ability to achieve very low levels of dopamine detection without requiring any electrode surface modification steps, a key factor in reducing fabrication costs and overall device complexity.

1. INTRODUCTION

Dopamine (DA) is a highly important neurotransmitter, produced in the ventral tegmental area, substantia nigra and hypothalamus areas of the brain [1]. DA is a catecholamine which plays a significant role in the function of various biological systems including renal [2], cardiovascular [3], hormonal [4] and central nervous [5] systems of mammals. DA can behave as both an excitatory or inhibitory neurotransmitter and acts as the brain's 'feel good' neurotransmitter. However, abnormal levels of DA play a role in different neurological disorders including depression [6], Parkinson's [7] and schizophrenia [8]. There exists a link between high DA levels and patients displaying symptoms of anxiety, aggression, mood swings, ADHD etc., whereas a lack of DA can lead to cognitive problems such as lack of energy, lack of motivation, poor concentration and difficulty in completing tasks [9]. Therefore, to be able to accurately diagnose conditions associated with DA dysfunction, effective and sensitive DA detection is critical, and is becoming an increasingly significant research area within the wider field of medicine and healthcare [10, 11].

To date, a range of DA detection methods have been investigated, to varying degrees of

success. Molecular imaging is one of the most commonly tested methods in the literature, and whilst it can be highly sensitive [12], it is also very expensive to implement and has the difficulty of being able to accurately separate DA from other key biological interferents such as ascorbic acid. On the other hand, electrochemical techniques have proven to be more cost-effective, sensitive, selective, and easier to implement into point of care systems [13-18]. The key parameters for a useful DA biosensor are high sensitivity and selectivity. It is well understood that the biomolecule ascorbic acid (AA) coexists in relatively high concentration in biological samples such as blood and urine, meaning that any detection method must be both sensitive and selective to DA and AA. AA is also known more commonly as vitamin C, and is found in various foods and dietary supplements. However, DA and AA oxidise at similar potentials resulting in interference in the electrochemical response. Therefore, there is a need for the development of a low-cost, sensitive, and highly selective sensor to DA using electrochemical techniques.

Previously, many methods have been adopted to try to detect DA using electrochemical approaches, with varying degrees of success. Often, electrodes are modified using a number of different materials to improve sensitivity and selectively compared to unmodified working electrodes. To avoid AA interference, overoxidised polypyrrole/graphene modified glassy carbon electrodes were fabricated [19]. The sensor displayed a linear response across a DA concentration range of 25 μM – 1 mM with a detection limit of 0.1 μM. Another electrode used to detect DA in the presence of AA and uric acid (UA) based on vanadium-substituted polyoxometalates, copper oxide and chitosan-palladium found good electrocatalytic activity toward DA oxidation, and displayed a limit of detection (LoD) of 45 pM [20]. A silver nanoparticle modified electrode covered by graphene oxide has been used to electrochemically

detect low concentrations of DA and produced a detection limit of 0.2 μM [21]. Despite the enhancement in sensitivity and selectivity afforded by these modified electrodes compared to the majority of bare electrodes, there is still room for improvement, particularly in terms of detection limit for DA, cost-effectiveness and ease of fabrication, with many of the reported electrode modifications being too impractical for manufacture.

One approach explored previously to detect DA is to use screen-printed electrodes (SPEs) to exploit their many advantages over more traditional electrodes such as simple fabrication and cleaning procedures, low cost, rapid time to result, reliability, and repeatability of measurements. They are also suitable for mass production, and large numbers of electrodes can be produced at reduced cost compared to traditional macro or microelectrodes [22]. However, the drawback of SPEs often lies in their ability to selectively detect DA alongside interferents such as AA, therefore they often require modification of the electrode surface, which adds additional complexity and cost to the fabrication process [23].

Our approach involves the use of a thin-film carbon-based flexible electrode (TFCE) defined by a dielectric which represents a relatively flat but disordered carbon surface, capable of detecting DA to low concentrations, as well as differentiating between DA and AA in solution, without the need for electrode surface modification. Having surveyed the literature, to the best of our knowledge this is the first report of DA detection in the presence of AA, without electrode surface modification, ultimately leading to a low cost and more manufacturable device suitable for mass production. Electrochemical techniques including cyclic voltammetry (CV) and differential pulse voltammetry (DPV) are used to characterise the electrodes as a function of DA concentration and to attempt to differentiate between DA and the common interferent AA. The electrode performance is also compared with a commercially available carbon SPE to evaluate

the best electrode configuration for sensitive and selective DA detection and to aid with design requirements for future TFCEs.

2. EXPERIMENTAL SECTION

2.1 Materials and Methods

Carbon-based thin-film electrodes (TFCEs) with a working electrode (WE) diameter of 1.09 mm were designed and produced in collaboration with FlexMedical Solutions Limited (Livingston, UK). Carbon screen printed electrodes (SPEs) encompassing reference and counter electrodes were obtained from DropSens (Oviedo, Spain) (ref 110). Examples of each electrode type are shown in Figures 1 (a) and (b).

All solutions were prepared with either 1xPBS (0.01 M) (phosphate buffered saline) or deionised (DI) water (Scientific Laboratory Supplies, Nottingham, UK). Sodium chloride (NaCl), dopamine hydrochloride (DA) and ascorbic acid (AA) were purchased from Sigma Aldrich (Dorset, UK).

Prior to measurement, all electrodes were cleaned using an electrochemical method involving immersion of the electrode in 20 mM NaCl and performing cyclic voltammetry (CV) across a potential range from 0 V to + 1.4 V at a sweep rate of 100 mV/s, for 10 cycles. After cleaning, the electrodes were rinsed with DI water and dried using compressed air.

2.2 Characterisation

All electrode measurements were performed using a three-electrode cell. Carbon SPEs are designed with the counter, reference and working electrodes together on a single chip, which eliminates the need to incorporate external counter and reference electrodes. TFCE measurements made use of an external platinum counter electrode and external saturated

Ag/AgCl reference electrode. All measurements were carried out using a potentiostat (Autolab PGSTAT204, Metrohm-Autolab, Utrecht, Netherlands). Measurements on DA detection were performed under ambient light conditions at room temperature.

DA and AA solutions were prepared in 1xPBS, and made up to a 1 mM concentration. Other concentrations were obtained from these 1 mM stock solutions and diluted to the desired concentration using 1xPBS.

CV measurements of DA and AA solutions were nominally performed by sweeping the potential between -0.3 V to 0.8 V with reference to the Ag/AgCl electrode three times. The third measurement was used for analysis. CV measurements were normalised with respect to working electrode area and shown as current density, *J*. Electrodes were characterised in the same measurement solution using differential pulse voltammetry (DPV) and some using square wave voltammetry (SWV). DPV and SWV were performed across the same potential range as CV. DPV/SWV measurements were also normalised with respect to working electrode area and shown as current density, *J*. Peak current densities (J_{pk}) from CV, DPV and SWV measurements were extracted as a function of DA/AA solution concentration. DPV and SWV data in some cases underwent a smoothing process to eliminate any electrical noise spikes in the data. For latter measurements performed as shown in Figures 3 and 4, linear baseline subtraction was performed on the data to eliminate any capacitance effects and to provide a better comparison between electrodes.

Scanning electron microscopy (SEM) (TM-1000, Hitachi, Tokyo, Japan) and atomic force microscopy (AFM) (Asylum Research MFP-3D, Abingdon, UK) images were taken of each electrode surface (TFCE and carbon SPE) to gain an impression of the individual surface profiles. SEM images were performed by scanning a 30 x 30 μm area, at a magnification of x 5.0

k. AFM images were performed using contact mode topography across a 7 x 7 μm area, and root-mean-square surface roughness (R_{RMS}) was extracted over three areas of each sample. Raman Spectroscopy was performed using a Raman microscope (Renishaw, inVia, Wotton-under-Edge, UK) featuring a 20/NA 0.40 objective and a 532 nm Nd:YAG laser. Raman spectra were obtained of the SPE and the TFCE across at least three samples to provide structural information about the carbon used in each electrode type.

3. RESULTS AND DISCUSSION

3.1 Electrodes

Figures 1 (a) and (b) show the two electrodes chosen for comparison, namely a 1.09 mm-diameter thin-film carbon electrode (TFCE) and a commercially available carbon screen-printed electrode (SPE) with a 4 mm working electrode (WE) diameter. The TFCE was fabricated by depositing a proprietary carbon screen printing ink onto a polyester substrate to a thickness of approximately 3 μm, and then using a polyester based ink to form the dielectric barrier, with the screen providing definition of the electrode and bond pad openings. The fabrication process results in a highly reproducible carbon layer from run-to-run, and each batch produces around 200 electrodes on one A4 sheet. The TFCE electrodes can be purchased from FlexMedical Solutions Limited (Livingstone UK). The SPE featuring dimensions 33 mm x 10 mm x 0.5 mm (length x width x height) consists of three main parts: a 4 mm-diameter carbon working electrode, a carbon counter electrode and a silver (Ag) reference electrode. The electrical contacts on the SPE are made of Ag. These electrodes have previously been used to study antibiotic resistance [24], oxygen gas detection in room-temperature ionic liquids [25] and to produce a disposable organophosphorus pesticides enzyme biosensor [26].

Each electrode surface was visualised using microscopy and surface profiling to investigate surface roughness. Figure 1 (c) shows scanning electron microscopy (SEM) images of the TFCE (i) and carbon SPE (ii) and atomic force microscopy (AFM) images of the TFCE (i) and SPE (ii) are shown in Figure 1 (d). When examined under SEM, the SPE displayed raised regions and significant non-uniformity compared to the relatively defect-free TFCE. From both SEM and AFM scans, it is clear that the TFCE has a smoother surface profile compared to the carbon SPE. R_{RMS} = 70.82 ± 1.63 nm for the TFCE, whereas the rougher SPE exhibited an RMS surface roughness of 136.05 ± 0.78 nm across the measured area. Figure 1 (e) (i) shows Raman spectra obtained from each electrode across a wavenumber range of ~ 100 to 3500 cm^{-1}. Figure 1 (e) (ii) shows the same data, this time between 1200 and 1800 cm^{-1} to enhance the clarity of the peaks, or carbon 'D' (disorder) and 'G' (graphite) bands. For both the SPE and TFCE, the spectra shown in Figure 1 (e) are indicative of amorphous carbon sp^2 [27] however, the intensity of the 'D' peak relative to the 'G' peak can be used to determine the degree of disorder within the sample [28]. It is clear that for both the SPE and the TFCE, the 'D' and 'G' bands appear at very similar wavenumbers, however, the intensity of the 'D' band over the 'G' band is greater for the SPE, with an intensity of 0.91 compared to 0.76 for the TFCE which is indicative of an improving amorphous structure of the carbon [29]. According to [29] which summarises the type of graphitic carbon, the TFCE carbon film is indicative of carbon materials produced by combustion based on the band shape, whereas the SPE carbon film is more akin to glassy carbon.

From the material characterisation techniques performed, it is clear that both the SPE and the TFCE feature a similar type of amorphous carbon. AFM images confirm that whilst the TFCE has a lower surface roughness than the SPE, Raman spectra indicate an increasing level of

disorder and defects for the TFCE which could be an indication of improved electrochemical performance for the TFCE's carbon layer [30].

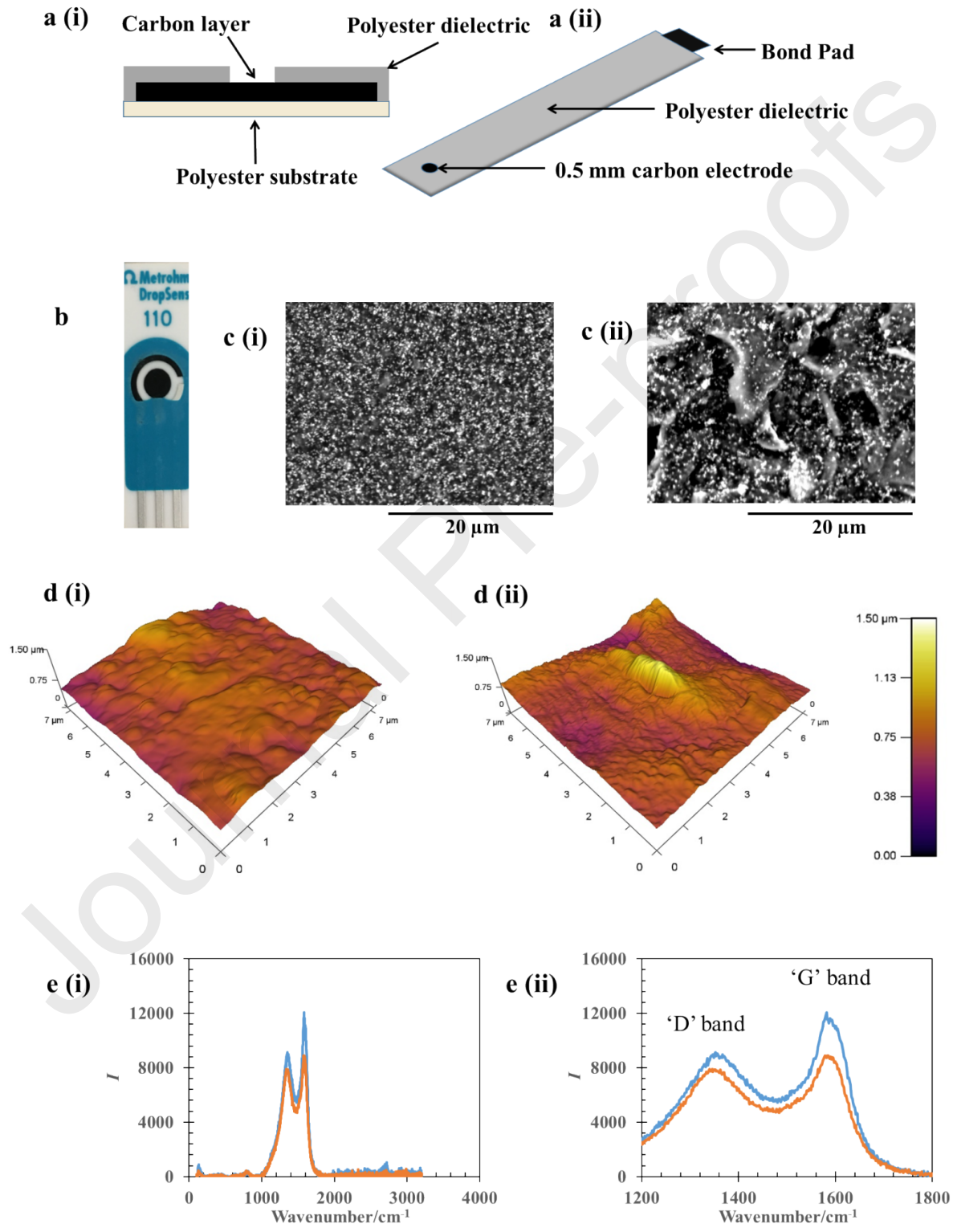

Figure 1. (a) 1.09 mm-diameter thin-film carbon electrode (TFCE). (i) Cross-section of electrode layers and (ii) 3D-representation of electrode geometry including carbon electrode, dielectric and bond pad. (b) Photograph of 4 mm-diameter carbon screen printed electrode (ref. 110). Also shown are the carbon counter electrode and silver reference electrode. (c) Scanning electron microscopy (SEM) images of TFCE (i) and carbon SPE (ii). (d) Atomic force microscopy (AFM) surface topography scans of TFCE (i) and carbon SPE (ii). (e) (i) Raman Spectra of the TFCE and carbon SPE between ~ 100 and 3500 wavenumber range and (ii) magnified Raman Spectra (1200-1800 (wavenumber range) for clarity. Labels for (e): TFCE (blue line), SPE (orange line). (For interpretation of the references to colour in this figure legend, the reader is referred to the web version of this article.)

3.2 DA Detection – Electrode Comparison

To investigate the effectiveness of our setup for DA detection, each electrode type was characterised side-by-side and a number of factors including CV and DPV response and CV and DPV scan rate were investigated to assess the best performing electrode. Figures 2 (a) (i) and (ii) show the CV response of the TFCE and SPE respectively to 1 mM-concentration DA solutions. It is clear that the current density is increased for the TFCE compared to the SPE. The TFCE produces a DA oxidation peak of 245 μA cm^{-2} at 0.5 V, compared to a peak of 105 μA cm^{-2} at 0.3 V for the SPE, an over two-fold increase. It should be noted that the peak voltages will differ between the two systems because of the use of an external Ag/AgCl (3.5 M) reference electrode for the TFCE measurements versus the on-board Ag electrode employed for the carbon SPE measurements. The corresponding DPV current density measurements for 1 mM DA are shown in Figures 2 (b) (i) and (ii) for each electrode. In this case, the oxidation voltage is reduced by ~ 0.1 V. J_{pk} = 48 and 90 μA cm^{-2} for the TFCE and SPE electrodes respectively, around a twofold difference for the SPE. However, this is likely attributable to differences in surface activity of the two electrodes as seen from Raman Spectroscopy. There is also significant background current in the DPV for the SPE compared to the TFCE. We attribute this high background to capacitive

currents from the SPE's overall higher surface area. It is therefore our hypothesis that whilst the electrode can store a high amount of charge, the lower surface activity of the material means the Faradaic current for dopamine is lower than for the TFCE. Critically, the TFCE shows the typical response for DA, i.e. a quasi-reversible voltammogram with the expected peaks for DA oxidation and reduction evident and present at voltages consistent with previous studies [31, 32]. By contrast, measurements from the carbon SPE exhibit significant capacitance in the CV response (see Figure 2 (a) (ii)) with the true quasi-reversible response being masked by this additional current. In addition, the DPV curve from the carbon SPE shows a significant background current (~75 μA cm^{-2}), again most likely still originating from capacitive effects despite employing DPV and therefore gives a compromised analytical performance.

The effect of CV and DPV scan rate is explored in Figure 2 (c) using the TFCE only to measure 1 mM DA. CV's were performed at 100 and 50 mV/s, and the DPV scan rate was investigated at 50, 10 and 5 mV/s. In each case, as the scan rate is reduced, the peak current density reduces too (as expected). For both CV and DPV measurements, the potential at which the peak occurs remains independent of scan rate, and therefore, provided the scan rate is consistent when comparing the two devices, the measurements of both CV and DPV will be reliable. Thus, a scan rate of 50 mV/s and 10 mV/s were chosen for all subsequent CV and DPV scans respectively.

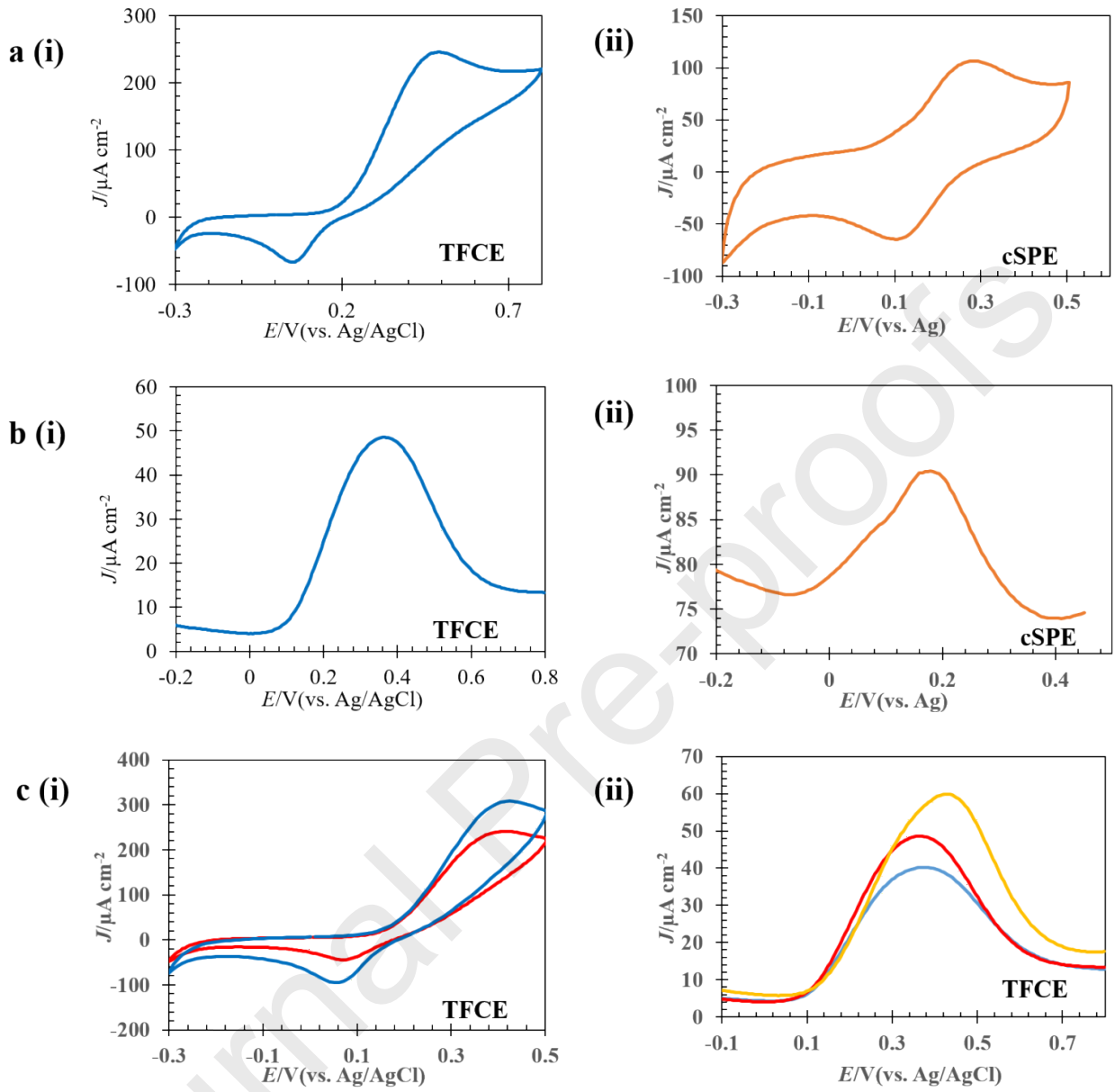

Figure 2. (a) CV current density of 1 mM-concentration DA solution measured using 1.09mm TFCE (i) and carbon SPE (ii) electrodes. (b) DPV current density of 1 mM-concentration DA measured using 1.09mm TFCE (i) and carbon SPE (ii) electrodes. (c) CV current density at different scan rates (100 mV/s: blue line, 50 mV/s: red line) (i) and DPV current density at different scan rates (5 mV/s: blue line, 10 mV/s: red line, 50 mV/s: yellow line) (ii) measuring 1 mM-concentration DA using TFCE. (For interpretation of the references to colour in this figure caption, the reader is referred to the web version of this article.)

3.3 DA Concentration Studies

To assess the sensitivity of each electrode type, the effect of DA concentration was investigated by measuring DPVs starting with a maximum concentration of 1 mM, and diluting the solution by a factor of 10 each time until a LoD could be estimated. DPV was chosen over CV as the electrochemical measurement technique of choice as a result of the improved sensitivity observed, particularly at lower DA concentrations for the TFCE. In addition, square wave voltammetry (SWV) was investigated as a potential measurement technique and equivalent DA concentration data measured using SWV is presented in the supporting information file (Figure S2). SWV was performed at an optimised frequency of 15 Hz as also displayed in the supporting information (Figure S1). Figure 3 (a) (i) shows the DPV measurements of different DA concentrations measured using the TFCE, with the equivalent measurements performed using a carbon SPE shown in Figure 3 (b) (i). For both electrode types, it is clear that as the concentration of DA is reduced, the peak current height reduces also, as expected. It is clear that the peak profile is more pronounced at 10 μM for the TFCE electrode compared to the SPE, indicating improved sensitivity of the TFCE at lower DA concentrations. To test this and to evaluate the limit of detection (LoD), the concentration of DA was further reduced and DPV measurements were taken. It was found that the LoD for the SPE was ~ 10 μM, since any DA concentration below this could not be faithfully resolved by DPV. However, the TFCE was still providing clear DPV current peaks as low as 50 pM DA, and these lowest resolvable concentrations are shown in Figures 3 (a) (ii) and 3 (b) (ii) for the TFCE and SPE respectively. Therefore, the LoD for the TFCE is significantly lower than the SPE (~ 6 orders of magnitude), which is important to be able to detect very low physiological concentrations of DA. In reality, it still proves challenging to accurately determine the concentration of extracellular DA in the

brain. Extracellular DA has been shown to affect postsynaptic neurons in the striatum in the brain [33] with current estimated concentrations of DA in the range of 5 to 50 nM. However, the synaptic concentration of DA is a function of different processes including release from terminals, metabolism and cellular uptake [34], and since release and uptake occur over rapid timescales, regulation of DA is a transient event and therefore the measurement time to obtain an accurate DA concentration for *in vivo* studies would be a critical factor for consideration. However, if estimates of DA concentration in the range of 5 to 50 nM are accurate as far as a rat model is concerned [33], then sensitivity down to tens of pM in solution as shown in this study should be suitable for physiological DA detection. A number of *in vivo* studies have been performed to varying degrees of success for dopamine detection. Through use of different electrode modification techniques including carbon nanotubes (CNTs) grown on microelectrodes and PEDOT/graphene oxide coating on carbon fiber electrodes [35, 36], sensitivity can certainly be improved, and in the case of the CNT method, DA limit of detection is in the nM range. Figure 3 (c) (i) shows the peak current density extracted from the DPV measurements performed as a function of DA concentration with the TFCE, with Figure 3 (d) displaying the DPV peak current density extracted for the SPE. For the lower concentration range of interest shown in Figure 3 (c) (ii), the TFCE produces a logarithmic response as a function of DA concentration from 100 nM to 50 pM, whereas from Figure 3 (d) the SPE J_{pk} produces a linear dependence as a function of DA concentration over the much narrower concentration range of 1 mM to 10 μM. Whilst a linear response is certainly a desirable trait, the sensitity of the TFCE over the SPE makes it a far superior sensor for DA detection.. The improved sensitivity exhibited by the TFCE electrode is not unsurprisng, since again, the WE surface area of the TFCE is reduced, meaning it will show improved sensitivity for DA detection. The poor sensitivity exhibited by the SPE

could imply either a saturation effect as DA concentration is reduced or be a result of *iR* drop (evident in unpublished results from our lab), whereby the commercial electrode cannot detect certain concentrations of DA well enough to be a useful sensor.

For each electrode, but in particular the TFCE, the DPV current density profiles at 1 mM are significantly greater than those at the lower concentrations, and do not appear to fit with the current scaling observed for the lower presented concentrations. When undertaking the experiments, the 1 mM-concentration DA formed a noticeable pink discolouration, whereas DA at all lower concentrations appeared colourless. This is due to the well known fact that DA undergoes oxidation to dopaminochrome, which is particulary noticeable when DA is concentrated and left in solution for a long period of time [37]. Dopaminochrome can have the effect of fouling the electrode and can also be a cause of lower than expected currents detected for very high concentrations of DA [38]. One way to counter this is to add a small amount of acid, as DA remains stable towards oxidation in acidic media, provided metal ions are absent. However, we decided not to add any acid in this study to maintain a situation resembling physiological conditions as much as possible. If looking to detect dopmine in the brain, the peripheral nervous system, the gut or directly in the blood, then to give a suitable proxy for an *ex vivo* meausurement, where controlling the pH environment would add additional complexity to an assay, it was decided not to acidify the DA solutions. Ultimately, this oxidation process did not appear to have any significant effect on the results since the DPV current appeared to scale suitably with regards to the lower and more physiologiclly relevant DA concentrations tested, and the DPV results overall indicate electroanalytical measurements can be performed suitably in unacidified solutions. Clearly, the addition of acid to the solution would enable a more stable biosensor response, however, on the scale of DA detection in a realistic

physiologocal situation, electrode stability will not be a major concern over such short measurement times.

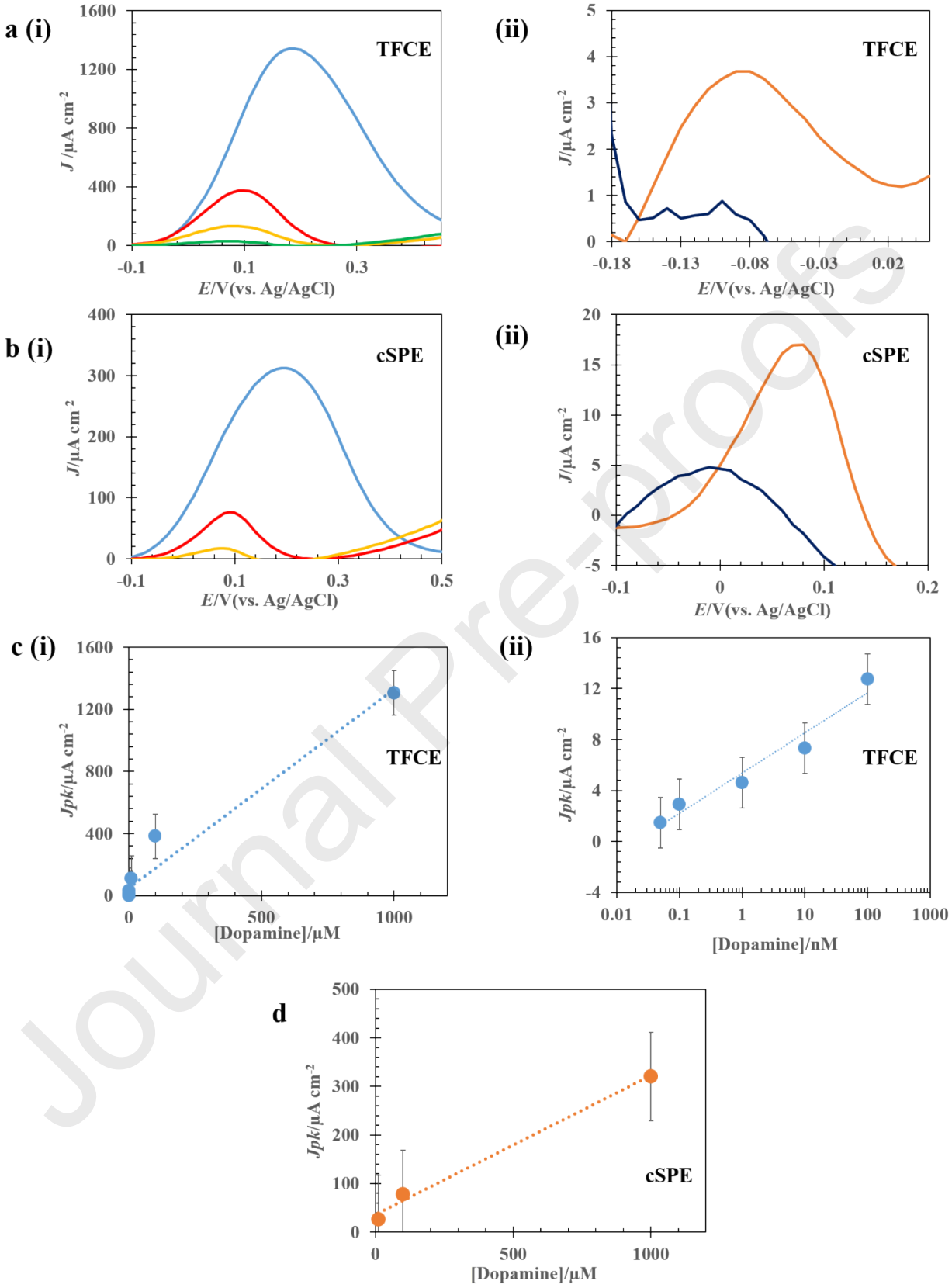

Figure 3. (a) (i) DPV (current density) measurements of different concentrations of DA measured using a 1.09mm-diameter TFCE (1 mM: blue line, 0.1 mM: red line, 10 μM: yellow line, 1 μM: green line). (ii) Lowest (50 pM) concentration of DA detected using DPV technique on TFCE (50 pM: orange line, 1xPBS: dark-blue line). (b) (i) DPV (current density) measurements of different concentrations of DA measured using a 4mm-diameter SPE (1 mM: blue line, 0.1 mM: red line, 10 μM: yellow line). (ii) Lowest (10 μM) concentration of DA detected using DPV technique on SPE (10 μM: orange line, 1xPBS: dark-blue line). (c) Peak DPV current density as a function of DA concentration measured with TFCE (i) and (ii) lower concentration range for clarity. (d) Peak DPV current density as a function of DA concentration measured with SPE. (For interpretation of the references to colour in this figure caption, the reader is referred to the web version of this article.)

3.4 Detection of Dopamine in the presence of the common interferent Ascorbic Acid

As a result of the promising data shown by the TFCE for low concentrations of DA, the electrode was investigated as a route to differentiate between not only DA, but DA combined with AA; a situation more closely resembling the physiological state [39]. To successfully demonstrate feasibility for the sensor, there has to exist a tangible difference between the electrochemical profiles of DA, AA, and both together. This could manifest itself as a difference in peak currents at the same potential, or preferably, a difference in oxidative potential, i.e. observable peak separation. Figure 4 (a) shows the CV (current density) (i) and DPV (current density) (ii) responses of the TFCE to 1 mM-concentration DA, 1 mM AA and 500 μM DA combined with 500 μM AA in order to evaluate the role AA plays in interfering with the DA electrochemical response. For comparison, the equivalent CV (current density) and DPV (current density) measurements taken using a carbon SPE are shown in Figure 4 (b). From both the CV and DPV measurements on the TFCE and SPE electrodes, DA produces a different electrochemical response to AA at the same concentration of 1 mM, i.e. voltages for oxidation potentials are different. From the CV measurements on the TFCE, DA gives a peak current

density of 326 μA cm^{-2} at a potential of 0.44 V, whereas AA gives a peak of 194 μA cm^{-2} at 0.59 V. Therefore, both the peak current density and potential separation can be used to identify DA in the presence of AA. This is confirmed when DA is combined with AA, the compounds in combination increase the overall current, and the CV and DPV curves show distinct peaks, 460 μA cm^{-2} at 0.44 V for DA and the other, 483 μA cm^{-2} at 0.58 V representing the contribution from AA. The DPV measurements confirm the same behaviour. The fact that both the peak current densities for DA and AA, and the fact there is an oxidative potential separation between them indicates the usefulness of the TFCE in being able to differentiate between DA and AA. Table 1 summarises the peak current densities and potentials for both the CV and DPV measurements performed on DA only, AA only and DA and AA using the TFCE.

In contrast, the commercially available SPE does not show such a significant difference between DA and AA, and for the DA + AA case, neither the CV (Figure 4 (b) (i)) nor DPV curves (Figure 4 (b) (ii)) show two distinct peaks representing DA and AA, unlike the TFCE. This confirms the improved sensitivity of the TFCE over the carbon SPE in its ability to distinguish between DA and AA.

However, in order to attempt to improve the selectivity of the TFCE for DA and AA detection, an alternative electrochemical technique (square wave voltammetry (SWV)) was tested to assess if it could increase the oxidative potential separation to ensure no overlap between the DA and AA peaks ultimately interfering with the overall response. SWV makes use of a combined square wave and staircase potential and has been found to be a highly sensitive technique for biosensor measurements [40, 41]. Supporting information Figure S1 shows the effect of (SWV) frequency on the peak current density measured for a fixed dopamine (DA) concentration of 500 μM. In this case, a frequency of 15 Hz was found to be optimal, and hence,

15 Hz was used for subsequent SWV measurements throughout the study. Figure 4 (c) (i) shows the response of the TFCE to 500 μM AA combined with different concentrations of DA (1 mM to 100 μM) to investigate the effect of SWV on the response. As expected, as the DA concentration decreases, the overall peak current reduces too. In addition, the peak potential separation is increased compared to the DPV data shown in Figure 4 (a) (ii). For example, in the case with both 500 μM AA and DA shown for clarity in Figure 4 (c) (ii), there is a clear DA peak at the lower potential value, ~ 0.15 V, whereas the peak for AA occurs around 0.48 V, a difference of ~ 0.33 V, significantly greater than the peak separation of ~ 0.11 V for the previous DPV measurement. This result is a positive one since it shows the potential of SWV to be used in place of CV or DPV to enhance the sensitivity of the TFCE system for DA detection in the presence of interferents including AA.

Table 2 summarises the peak current densities and potentials for the SWV data on the TFCE shown in Figure 4 (c).

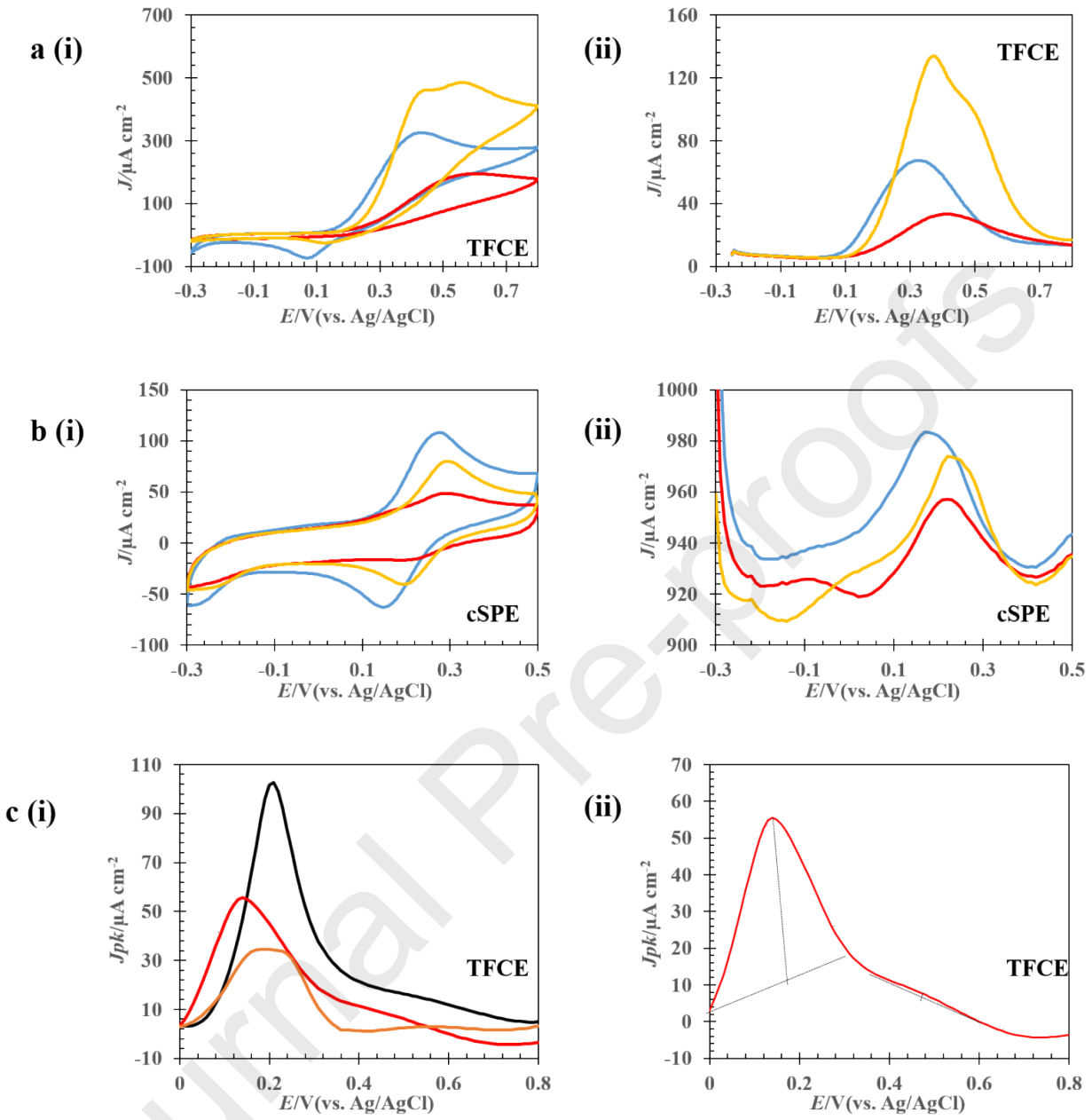

Figure 4. (a) CV (current density) (i) and DPV (current density) (ii) measurements of 1 mM-concentration DA, AA and DA + AA measured using TFCE. (b) CV (current density) (i) and DPV (current density) (ii) measurements of 1 mM-concentration DA, AA and DA +AA measured using 4 mm-diameter carbon SPE. (Labels for (a) and (b): DA Only: blue line, AA Only: red line, DA + AA: yellow line). (c) SWV (current density) measurements of 500 µM-concentration AA combined with different concentrations of DA (1 mM: black line, 500 µM: red line, 100 µM: orange line). (ii) shows the 500 µM AA + 500 µM-concentration DA case for clarity and relevance of CV and DPV

data shown. (For interpretation of the references to colour in this figure caption, the reader is referred to the web version of this article.)

Table 1. Peak current densities and corresponding voltages from CV and DPV measurements on 1 mM DA, AA and DA+AA measured on TFCE.

CV	J_{pk} / μA cm^{-2}	E / V	DPV	J_{pk} / μA cm^{-2}	E / V
DA Only	325.83	0.44	DA Only	67.41	0.33
AA Only	194.00	0.59	AA Only	33.20	0.42
DA + AA (Two peaks)	459.81, 483.39	0.44, 0.58	DA + AA (Two peaks)	133.0, 100.45	0.38, 0.49

Table 2. Peak current densities and corresponding voltages from SWV measurements on 500 μM AA combined with different concentrations of DA measured on TFCE.

1 mM DA	J_{pk} / μA cm^{-2}	E /V	500 μM DA	J_{pk} / μA cm^{-2}	E / V	100 μM DA	J_{pk} / μA cm^{-2}	E / V
DA Peak	102.52	0.21	DA Peak	55.04	0.15	DA Peak	34.34	0.21
AA Peak	13.38	0.57	AA Peak	7.28	0.48	AA Peak	2.96	0.57

The data presented above represent a first demonstration of the ability of the sensor to discriminate between DA and AA and these initial measurements were performed with a relative abundance of DA in solution and with relatively unoptimised DPV and SWV wave forms. Recent work has shown that electrochemical biosensor sensitivity can be dramatically enhanced through matching the frequency of in particular a SWV waveform to the rate constant for the redox system under test [42]. We therefore feel there is significant room for optimisation with this system and to push the dopamine sensitivity in solutions of DA spiked with AA and then finally in physiological solutions such as blood. Due to the sensor design and the flexible nature of the device, we feel it is more suitable for *ex vivo* measurement of DA, such as in blood and perhaps for use in DA sensing in the gut where bacteria are known to produce around 50% of the body's DA pool. With links emerging between the enteric nervous system, the microbiome and the production and maintenance of the physiological DA pool, we believe this low-cost sensor could find use in such measurements. We believe there are other more suitable sensors for direct measurement in the brain such as microfabricated systems.

Finally, it is worth pointing out that the TFCE is capable of being reused repeatedly without significant loss in sensitivity. Unlike many other forms of biosensor whereby surface modification or attachment of a receptor to the sensor surface render it a 'one-use' device, the TFCE simply measures DA in solution, and upon simple electrochemical CV cleaning in a low concentration (20 mM) solution of NaCl, any residual DA on the electrode surface is removed, enabling the electrode to be reused a number of times, vastly reducing what is already low fabrication cost (<£2 per device).

4 CONCLUSIONS

A carbon, thin-film flexible electrode has been shown as a useful, low-cost biosensor, capable of detecting important neurotransmitter DA using the electrochemical techniques of cyclic voltammetry and differential pulse voltammetry. The voltammetric responses of the device confirmed the successful production of a sensor with complete passivation of the underlying insulator, therefore giving rise to a well-defined electrode surface which could be used to perform analytical measurements. The behaviour of the TFCE was compared to a commercially available screen printed electrode. It was found that the TFCE was more sensitive than the SPE with significantly reduced background currents (most likely arising from capacitive effects), and was able to detect DA in solution down to ~ 50 pM. In addition, the TFCE was used to discriminate between DA in the presence of the key interferent AA to reflect a more realistic physiological situation. In this case, when examined using CV or DPV, the electrode was able to show a difference in DA current density peak as well as oxidative potential at 500 μM concentration, two possible markers to be able to clearly differentiate between the different compounds. Furthermore, by exploring the analytical technique of SWV, the selectivity of the TFCE for DA detection in the presence of AA could be improved since SWV led to an increased peak potential separation between DA and AA signals. This selectivity between these two compounds is in contrast to the commercially available carbon screen printed electrode, which failed to distinguish between DA and AA. Furthermore, when examined under SEM and AFM, the TFCE displayed a relatively disordered carbon surface, with a low surface roughness. In comparison, the SPE featured a rougher surface profile, resulting in a larger surface roughness with Raman studies showing lower defectivity. The improved performance of the TFCE device is largely explained in terms of the morphology and defectivity of the carbon surface, with lower surface roughness giving rise to a more consistent surface area (device to device) with the higher

density of defects giving enhanced electron transfer rates across the surface compared to the screen printed sensor. The key advantages of our TFCE device are that it is cost-effective, flexible, mass-manufacturable, does not require any WE surface modification, and is proven to be both highly sensitive to DA and able to discriminate between DA and the common interferent AA. To the best of our knowledge, this is one of the lowest LoDs for DA (~ 50 pM) reported to date using a non-modified carbon-based electrode. Going forward, a device such as the TFCE could be envisaged for use *in* and *ex vivo*, to monitor behaviour of DA within the blood and peripheral and enteric nervous systems to provide a useful system for rapid and sensitive physiological DA detection in a clinical setting. Future work will involve testing in blood and optimisation of the DPV and SWV scan parameters to determine if DA sensitivity can be further enhanced.

ACKNOWLEDGMENTS

DC would like to acknowledge the Fast-tracking Health Innovation for NHS Scotland. MRC Confidence in Concept Scheme/R180246-103 for financial support. TFCEs were developed and supplied by FlexMedical Solutions Limited, Livingston, UK. We acknowledge Dr Milovan Cardona (Biomedical Engineering, University of Strathclyde, UK) for SEM and AFM imaging support and Dr Will Tipping (Pure & Applied Chemistry, University of Strathclyde, UK) for Raman Spectroscopy support.

AUTHOR INFORMATION

Corresponding Author

*(D.C) E-mail: damion.corrigan@strath.ac.uk

Credit Author Statement

Stuart Hannah: Formal analysis, Investigation, Methodology, Project administration, Supervision, Validation, Visualisation, Writing – original draft, Writing – review and editing. **Maha Al-Hatmi:** Methodology, Formal analysis, Investigation, Methodology, Validation. **Louise Gray:** Resources. **Damion Corrigan:** Conceptualization, Formal analysis, Funding acquisition, Investigation, Methodology, Project administration, Resources, Supervision, Validation, Visualization, Writing – review and editing.

COMPETING INTERESTS

The authors declare they have no competing interests, whether financial or otherwise.

REFERENCES

[1] Olguin, H. J.; Guzman, D. C.; Garcia, E. H.; Mejia, G. B. The Role of Dopamine and its Dysfunction as a Consequence of Oxidative Stress. *Oxidative Medicine and Cellular Longevity*. **2015,** *2016,* 1-13.

[2] Choi, M. R.; Kouyoumdzian, N. M.; Mikusic, N. L. R.; Kravetz, M. C.; Roson, M. I.; Fermepin, M. R.; Fernandez, B. E. Renal Dopaminergic System: Pathophysiological Implications and Clinical Perspectives. *World. J. Nephrol*. **2015,** *4,* 196-212.

[3] Setler, P. E.; Pendleton, R. G.; Finlay, E. The Cardiovascular Actions of Dopamine and the Effects of Central and Peripheral Catecholaminergic Receptor Blocking Drugs. *J. Pharmacol. Exp. Ther*. **1975,** *192,* 702-712.

[4] Ugriumov, M. V. Endocrine Functions of the Brain in Adult and Developing Mammals. *Ontogenez*. **2009,** *40,* 19-29.

[5] Jaber, M.; Robinson, S. W.; Missale, C.; Caron, M. G. Dopamine Receptors and Brain Function. *Neuropharmacology*. **1996,** *35,* 1503-1519.

[6] Tye, K. M..; Mirzabekov, J. J.; Warden, M. R..; Ferenczi, E. A.; Tsai, H. C.; Finkelstein, J.; Kim, S. Y.; Adhikari, A.; Thompson, K. R.; Andalman, A. S.; Gunaydin, L. A.; Witten, I. B.; Deisseroth, K. Dopamine Neurons Modulate Neural Encoding and Expression of Depression-Related Behaviour. *Nature*. **2013,** *493,* 537-541.

[7] Dalley, J. W..; Roiser, J. P. Dopamine, Serotonin and Impulsivity. *Neuroscience*. **2012,** *215,* 42-58.

[8] Brisch, R.; Saniotis, A.; Wolf, R.; Bielau, H.; Bernstein, H. G.; Steiner, J.; Bogerts, B.; Braun, K.; Jankowski, Z.; Kumaratilake, J.; Henneberg, M.; Gos, T. The Role of Dopamine in Schizophrenia from a Neurobiological and Evolutionary Perspective: Old Fashioned, but Still in Vogue. *Front Psychiatry*. **2014,** *5,* 1-11.

[9] Dobryakova, E.; Genova, H. M.; DeLuca, J.; Wylie, G. R. The Dopamine Imbalance Hypothesis of Fatigue in Multiple Sclerosis and Other Neurological Disorders. *Front Neurol*. **2015,** *6,* 1-8.

[10] Choo, S. S.; Kang, E. S.; Song, I.; Lee, D.; Choi, J. W.; Kim, T. H. Electrochemical Detection of Dopamine Using 3D Porous Graphene Oxide/Gold Nanoparticle Composites. *Sensors (Basel)*. **2017,** *17,* 861.

[11] Zhang, X.; Chen, X.; Kai, S.; Wang, H. Y.; Yang, J.; Wu, F. G.; Chen, Z. Highly Sensitive and Selective detection of Dopamine Using One-Pot Synthesised Highly Photoluminescent Silicon Nanoparticles. *Anal. Chem*. **2015,** *87,* 3360-3365.

[12] Badgaiyan, R. D. Imaging Dopamine Neurotransmission in Live Human Brain. *Prog. Brain Res*. **2014,** *211,* 165-182.

[13] Kumar, P. S.; Megarajan, S.; Reddy, G. R. K.; Anbazhagan, V. Facile Synthesis of Gold Nanoparticles Using Carbon Dots for Electrochemical Detection of Neurotransmitter, Dopamine in Human Serum and as a Chemocatalyst for Nitroaromatic Reduction. *IET Nanobiotechnology*. **2018,** *12,* 909-914.

[14] Wu, L.; Feng, L.; Ren, J.; Qu, X. Electrochemical Detection of Dopamine Using Porphyrin-Functionalised Graphene. *Biosensors and Bioelectronics*. **2012,** *34,* 57-62.

[15] Cheng, Q.; Wang, H.; Wu, Y.; Zhao, S.; Kong, X.; Chen, Y.; Jiang, J. Highly Selective Enzymatic-Free Electrochemical Sensor for Dopamine Detection Based on the Self-Assemblied Film of a Sandwich Mixed (Phthalocyaninato) (Porphyrinato) Europium Derivative. *J. Porphyrins and Phthalocyanines*. **2017,** *21,* 796-802.

[16] Kim, D. S.; Kang, E. S.; Baek, S.; Choo, S. S.; Chung, Y. H.; Lee, D.; Min, J.; Kim, T. H. Electrochemical Detection of Dopamine Using Periodic Cylindrical Gold Nanoelectrode Arrays. *Sci. Rep*. **2018,** *8,* 14049.

[17] Fayemi, O. E.; Adekunle, A. S.; Swamy, B. E. K.; Ebenso, E. E. Electrochemical Sensor for the Detection of Dopamine in Real Samples Using Polyaniline/NiO, ZnO, and Fe_3O_4 Nanocomposites on Glassy Carbon Electrode. *J. Anal. Chem*. **2018,** *818,* 236-249.

[18] Khan, M. Z. H. Graphene Oxide Modified Electrodes for Dopamine Sensing. *J. Nanomat*. **2017,** *2017,* 1-11.

[19] Zhuang, Z.; Li, J.; Xu, R.; Xiao, D. Electrochemical Detection of Dopamine in the Presence of Ascorbic Acid Using Overoxidised Polypyrrole/Graphene Modified Electrodes. *Int. J. Electrochem. Sci*. **2011,** *6,* 2149-2161.

[20] Zhang, L.; Ning, L.; Li, S.; Pang, H.; Zhang, Z.; Ma, H.; Yan, H. Selective Electrochemical Detection of Dopamine in the Presence of Uric Acid and Ascorbic Acid Based on a Composite Film Modified Electrode. *RSC Advances*. **2016,** *6,* 66468-66476.

[21] Shin, J. W.; Kim, K. J.; Yoon, J.; Jo, J.; El-Said, W. A.; Choi, J. W. Silver Nanoparticle Modified Electrode Covered by Graphene Oxide for the Enhanced Electrochemical Detection of Dopamine. *Sensors (Basel)*. **2017,** *17,* 2771-2781.

[22] Hayat, A.; Marty, J. L. Disposable Screen Printed Electrochemical Sensors: Tools for Environmental Monitoring. *Sensors*. **2014,** *14,* 10432-10453.

[23] Redin, G. I.; Wilson, D.; Goncalves, D.; Oliveira Jr., O. N. Low-Cost Screen-Printed Electrodes Based on Electrochemically Reduced Graphene Oxide-Carbon Black Nanocomposites for Dopamine, Epinephrine and Paracetamol Detection. *J. Colloid and Interface. Sci*. **2018,** *515,* 101-108.

[24] Obaje, E. A.; Cummins, G.; Schulze, H.; Mahmood, S.; Desmulliez, M. P. Y.; Bachmann, T. T. Carbon Screen-Printed Electrodes on Ceramic Substrates for Label-Free Molecular Detection of Antibiotic Resistance. *J. Interdisciplinary. Nanomed*. **2016,** *1*.

[25] Lee, J.; Hussain, G.; Banks, C. E.; Silvester, D. S. Screen-Printed Graphite Electrodes as Low-Cost Devices for Oxygen Gas Detection in Room-Temperature Ionic Liquids. *Sensors (Basel)*. **2017,** *17,* 2734-2747.

[26] Gan, N.; Yang, X.; Xie, D.; Wu, Y.; Wen, W. A Disposable Organophosphorus Pesticides Enzyme Biosensor Based on Magnetic Composite Nano-Particles Modified Screen Printed Carbon Electrode. *Sensors*. **2010,** *10,* 625-638.

[27] Schwan, J.; Ulrich, S.; Batori, V.; Ehrhardt, H.; Silva, S. R. P. Raman Spectroscopy on Amorphous Carbon Films. *J. Appl. Phys*. **1996,** *80,* 440-447.

[28] Dillon, R. O.; Woollam, J. A.; Katkanant, V. Use of Raman Scattering to Investigate Disorder and Crystallite Formation in As-Deposited and Annealed Carbon Films. *J. Mater. Res* **1984,** *29,* 3482-3489.

[29] Knight, D. S.; White, W. B. Characterisation of Diamond Films by Raman Spectroscopy. *Phys*. *Rev. B* **1989,** *4,* 385-393.

[30] Martin-Yerga, D.; Costa-Garcia, A.; Unwin, P. R. Correlative Voltammetric Microscopy: Structure-Activity Relationships in the Microscopic Electrochemical Behavior of Screen Printed Carbon Electrodes. *ACS. Sens.* **2019,** *4,* 2173-2180.

[31] Khan, N. F.; Brownson, D. A. C.; Randviir, E. P.; Smith, G. C.; Banks, C. E. 2D Hexagonal Boron Nitride (2D-hBN) Explored for the Electrochemical Sensing of Dopamine. *Anal. Chem*. **2016,** *88,* 9729-9737.

[32] Corona-Avendano, S.; Alarcon-Angeles, G.; Ramirez-Silva, M. T.; Rosquete-Pina, G.; Romero-Romo, M.; Palomar-Pardave, M. On the Electrochemistry of Dopamine in Aqueous Solution. Part I: The Role of [SDS] on the Voltammetric Behaviour of Dopamine on a Carbon Paste Electrode. *J. Electroanal. Chem*. **2007,** *609,* 17-26.

[33] Kawagoe, K. T.; Garris, P. A.; Wiedemann, D. J.; Wightman, R. M. Regulation of Transient Dopamine Concentration Gradients in the Microenvironment Surrounding Nerve terminals in the Rat Striatum. *Neuroscience*. **1992,** *51,* 55-64.

[34] Justice, J. B. Jr.; Nicolaysen, L. C.; Michael, A. C. Modeling the Dopaminergic Nerve Terminal. *J. Neurosci. Methods*. **1988,** *22,* 239-252.

[35] Yang, C.; Jacobs, C. B.; Nguyen, M. D.; Ganesana, M.; Zestos, A. G.; Ivanov, I. N.; Puretzky, A. A.; Rouleau, C. M.; Geohegan, D. B.; Venton, B. J. Carbon Nanotubes Grown on Metal Microelectrodes for the Detection of Dopamine. *Anal. Chem*. **2016,** *88,* 645-652.

[36] Taylor, I. M.; Robbins, E. M.; Catt, K. A.; Cody, P. A.; Happe, C. L.; Cui, X. T. Enhanced Dopamine Detection Sensitivity by PEDOT/graphene Oxide Coating on *in vivo* Carbon Fiber Electrodes. *Biosensors & Bioelectronics*. **2017,** *89,* 400-410.

[37] Herlinger, E.; Jameson, R. F.; Linert, W. Spontaneous Autoxidation of Dopamine. *J. Chem. Soc. Perkin. Trans*. **1995,** *2,* 259-263.

[38] Harreither, W.; Trouillon, R.; Poulin, P.; Neri, W.; Ewing, A. G.; Safina, G. Carbon Nanotube Fiber Microelectrodes show a Higher Resistance to Dopamine Fouling. *Anal. Chem.* **2013,** *85,* 7447-7453.

[39] Naik, R. R..; Swamy, B. E. K.; Chandra, U.; Niranjana, E.; Sherigara, B. S.; Jayadevappa, H. Separation of Ascorbic Acid, Dopamine and Uric Acid by Acetone/Water Modified Carbon Paste Electrode: A Cyclic Voltammetric Study. *Int. J. Electrochem. Sci.* **2009,** *4,* 855-862.

[40] Kinnamon, D.; Muthukumar, S.; Selvam, A. P.; Prasad, S. Portable Chronic Alcohol Consumption Monitor in Human Sweat through Square-Wave Voltammetry. *SLAS Technol.* **2018,** *23*, 144-153.

[41] Rassas, I.; Braiek, M.; Bonhomme, A.; Bessueille, F.; Raffin, G.; Majdoub, H.; Jaffrezic-Renault, N. Highly Sensitive Voltammetric Glucose Biosensor Based on Glucose Oxidase Encapsulated in a Chitosan/Kappa-Carrageenan/Gold Nanoparticle Bionanocomposite. *Sensors*. **2019**, *19*, 154.

[42] Dauphin-Ducharme, P.; Plaxco, K. W. Maximizing the Signal Gain of Electrochemical-DNA Sensors. *Anal*. *Chem.* **2016,** *88,* 11654-11662.

GA

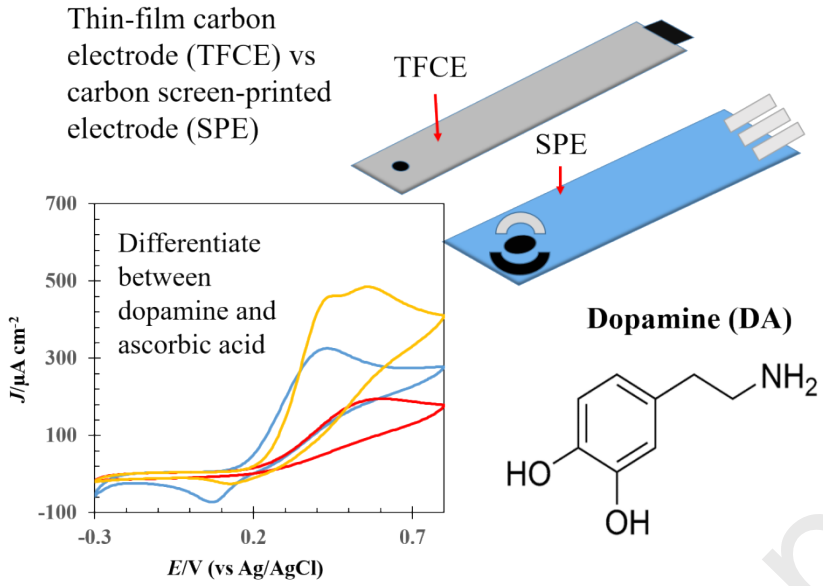

- A flexible, thin-film carbon electrode developed for detection of dopamine.
- The electrode was electrochemically characterised to assess its sensitivity.
- The electrode provided a dopamine limit of detection of ~ 50 pM.
- Good selectivity shown between dopamine and key interferent, ascorbic acid.

Conflict of Interest and Authorship Conformation Form

Please check the following as appropriate:

- All authors have participated in (a) conception and design, or analysis and interpretation of the data; (b) drafting the article or revising it critically for important intellectual content; and (c) approval of the final version.
- This manuscript has not been submitted to, nor is under review at, another journal or other publishing venue.
- The authors have no affiliation with any organization with a direct or indirect financial interest in the subject matter discussed in the manuscript

Author's name	Affiliation
Stuart Hannah	Department of Biomedical Engineering, University of Strathclyde, 40 George Street, Glasgow, G1 1QE, United Kingdom.
Maha Al-Hatmi	Department of Biomedical Engineering, University of Strathclyde, 40 George Street, Glasgow, G1 1QE, United Kingdom.
Louise Gray	FlexMedical Solutions, Eliburn Industrial Park, Livingston, EH54 6GQ, United Kingdom.
Damion K Corrigan	Department of Biomedical Engineering, University of Strathclyde, 40 George Street, Glasgow, G1 1QE, United Kingdom.